REVERSE ANNEALING IN RADIATION-DAMAGED, SILICON SOLAR CELLS

Irving Weinberg and Clifford K. Swartz
National Aeronautics and Space Administration
Lewis Research Center

INTRODUCTION

The phenomenon of reverse annealing has been observed in bulk silicon (ref. 1) and in silicon solar cells (refs. 2 and 3). To date, however, attempts to understand this detrimental effect, in terms of the defects formed by particulate radiation, have been unsuccessful. Recently, however, sensitive instrumental techniques have been used to gain increased insight into the behavior of defects formed in p-type silicon by particulate radiation (refs. 4-7). Hence, in the present work, we report results using relatively new information regarding defect formation in boron doped silicon (refs. 6 and 7) in calculations which tend to clarify and explain the reverse annealing effects we observe in silicon solar cells.

EXPERIMENTAL

Irradiations and isochronal annealing were performed on n^+p silicon solar cells with 0.1 and 2 ohm-cm boron doped base resistivities. Starting material for the 2 ohm-cm cell was Czochralski grown while the starting material for the .1 Ω-cm cell was vacuum float zone single crystal silicon. The cells were irradiated by 1 Mev electrons to a fluence of 10^{15} cm^{-2}. After irradiation, the cells were isochronally annealed in 50° C steps, the cells being held at each fixed temperature point for 20 minutes. Minority carrier diffusion lengths and AMO I-V measurements were obtained at room temperature before and after irradiation and after each step in the isochronal anneal. Diffusion lengths were measured by an X-ray excitation technique (ref. 8), while the AMO I-V measurements were obtained using a xenon-arc solar simulator. Isochronal annealing data are shown in figure 1 where it is seen that reverse annealing occurs for the 2 ohm-cm cell at temperatures above 150° C, but is absent in the 0.1 ohm-cm cell's data.

In order to understand these results in terms of properties of the radiation induced defects, we used a combination of our diffusion length measurements and defect data obtained from Deep Level Transient Spectroscopy (DLTS), (ref. 7). The pertinent diffusion length data for the cells of figure 1 are shown in figure 2, where L_T^{-2} is reciprocal diffusion length squared, measured at room temperature after isochronal anneal at temperature T, while L_{IRR}^{-2} is

reciprocal diffusion length squared measured at room temperature after irradiation and before annealing. The DLTS, isochronal annealing data for a 2 ohm-cm n^+p silicon solar cell are shown in figure 3, while figure 4 shows the DLTS data for a 0.3 ohm-cm cell (ref. 7). In figures 3 and 4, E_v is energy at the top of the valence band, while E_c is energy at the bottom of the conduction band. Regarding the cells used to obtain the DLTS data (ref. 7), starting material for the 2 Ω-cm cell was Czochalski grown boron-doped silicon, while that for the 0.3 Ω-cm cell was vacuum float zone boron-doped silicon.

THEORY

Derivation of Working Equation

To obtain an equation relating the present diffusion length data to defect parameters, such as carrier capture cross sections and relative defect concentrations, we use the Shockley-Read-Hall (SRH) theory of recombination (refs. 9 and 10). Our starting point is the SRH expression for τ_i the carrier lifetime due to the i^{th} single level defect. For low injection conditions we have (refs. 9 and 10)

$$\frac{1}{\tau_i} = \frac{N_i}{\frac{1}{v_p \sigma_{pi}}\left(\frac{n_o+n_1}{n_o+p_o}\right) + \frac{1}{v_n \sigma_{ni}}\left(\frac{p_o+p_1}{n_o+p_o}\right)} \tag{1}$$

Where N_i is the concentration of the i^{th} defect, n_o and p_o are equilibrium electron and hole concentrations, v_n and v_p are thermal velocities for electrons and holes, σ_{pi} and σ_{ni} are hole and electron capture cross sections for the i^{th} defect and n_i and p_i are calculated from the relations

$$n_1 = N_c \exp\left(\frac{E_i - E_c}{kT}\right) \tag{2a}$$

$$p_1 = N_v \exp\left(\frac{E_v - E_i}{kT}\right) \tag{2b}$$

Where N_c and N_v are the density of states for the conduction and valence bands k is the Boltzmann constant and Ei is the energy level of the i^{th} defect. The thermal velocities are obtained from the relations

$$v_p = \left(\frac{3kT}{m_h}\right)^{1/2} \tag{3a}$$

$$v_n = \left(\frac{3kT}{m_e}\right)^{1/2} \tag{3b}$$

Where m_h and m_e are hole and electron effective masses respectively.

For P type silicon p_o is measured and n_o calculated from the relation

$$n_o p_o = n_I^2 \tag{4}$$

Where n_I is the intrinsic carrier concentration.

Using equations 2, 3 and 4, we find for the defects in figures 3 and 5 that

$$\frac{p_o + p_1}{n_o + p_o} \approx 1$$

$$\frac{n_o + n_1}{n_o + p_o} \ll 1 \text{ , and}$$

$$v_n \approx v_p \approx 2 \times 10^7 \text{ cm/sec.}$$

Hence equation 1 simplifies to

$$\frac{1}{\tau_i} \approx N_i \sigma_{ni} v_n = N_{max} R_i \sigma_{ni} v_n \tag{5}$$

Where R_i is the relative concentration of the i^{th} defect with

$$R_i = \frac{N_i}{N_{max}} \tag{6}$$

N_{max} being the maximum defect concentration measured by DLTS during the isochronal anneal. For example in figure 3, N_{max} is obtained from the peak amplitude of the E_v + .38 defect (ref. 7).

Since

$$\frac{L_T^{-2}}{L_{IRR}^{-2}} = \frac{\left(\frac{1}{\tau}\right)_T}{\left(\frac{1}{\tau}\right)_{IRR}} = \frac{\left(\sum_i \frac{1}{\tau_i}\right)_T}{\left(\sum_i \frac{1}{\tau_i}\right)_{IRR}} \tag{7}$$

We obtain the required relation

$$\frac{L_T^{-2}}{L_{IRR}^{-2}} \approx \frac{\left(\sum_i R_i \sigma_{ni}\right)_T}{\left(\sum_i R_i \sigma_{ni}\right)_{IRR}} \tag{8}$$

Capture Cross Section

The capture cross sections obtained from DLTS (ref. 7), are listed in Table 1. Since the electron capture cross section σ_n for only one defect (E_c-0.27 eV) is available from DLTS, we cannot calculate diffusion length ratios from equation 8 using only this DLTS result. We have therefore obtained the necessary additional σ_n values by other methods.

With respect to the defects at E_v+0.38 and E_v+0.23, temperature dependent lifetime studies in 1.5 ohm-cm p-type silicon yield values for the ratio σ_n/σ_p from which σ_n is calculated (ref. 11). From reference 11, for the E_v+0.38 defect $\sigma_n/\sigma_p \approx 150$ and for the defect at E_v+0.23, $\sigma_n/\sigma_p \approx 1300$ from which the σ_n values for these defects shown in Table 2 are calculated. For the remaining defects, values for σ_n were computed by fitting equation 8 to the diffusion length data of figure 2 at 250 and 300° C using R_i values from figure 3. In this way, the electron capture cross sections for the defects at E_v+0.30 and E_v+0.26 were obtained. Thus, the required cross sections for all but the defect at E_v+0.2 eV are obtained for use in equation 8. Since we cannot evaluate σ_n for this latter defect, it is arbitrarily assumed that it can be ignored in subsequent calculations. Similar considerations apply to the E_v+0.48 defect in 0.3 ohm-cm p-silicon (fig. 4) i.e., since we cannot evaluate σ_n for this defect it is omitted from the calculations.

RESULTS

The L^{-2} ratios, for the 2 Ω-cm cell, calculated from equation 8, using relative concentrations from figure 3 and capture cross sections from Table 2 are shown in figure 5. From the figure it is seen that the calculated and measured values are in reasonable agreement. From these results, the defect responsible for the reverse annealing in 2 ohm-cm p-type silicon is identified as the defect at E_V+0.30 eV. Additional calculations were performed after conceptually removing this defect, using the remaining cross sections of Table 1 and the remaining relative concentrations of figure 3. The result is shown in figure 6.

Calculated values for the 0.3 ohm-cm cell using the data of Table 2 and figure 4 are shown in figure 7. These results indicate the absence of reverse annealing in this low resistivity cell and are in qualitative agreement with our data for the 0.1 ohm-cm cell. Removal of the E_V+0.30 defect results in calculated values shown by the dotted line of figure 7. Since no DLTS data are available for 0.1 ohm-cm p-type silicon, we interpret these 0.3 ohm-cm results as an indication of trends when going to lower resistivity p-type silicon.

DISCUSSION

The good agreement between our experimental and calculated values indicates the correctness of the mathematical relationship (equation 8) derived from the SRH theory. Our results indicate that the defect at E_V+0.30 eV is responsible for the observed reverse annealing. Furthermore, its removal could result in significant annealing at 200° C for the cells investigated. Since the E_V+0.30 defect always appears when the E_C-0.27 defect disappears (ref. 7) the two defects are related in the sense that the E_C-0.27 defect can be called the "parent" to the E_V+0.30 defect. Hence, the atomic constitution of both defects is of importance.

The defect at E +0.30 has been tentatively identified as a boron-oxygen-vacancy complex (ref. 7). The E_C-0.27 defect increases in concentration with increasing boron concentration and has been identified as a boron interstitial-oxygen interstitial complex (ref. 7). An alternate identification asserts that the E_C-0.27 defect is composed of a boron interstitial-boron substitutional pair (ref. 12). A firmer identification of the E_V+0.30 defect is required as well as additional research directed at choosing between competing identifications for the E_C-0.27 parent defect. Such identifications would be an invaluable guide to processing efforts aimed at decreasing the concentration of these radiation induced defects.

REFERENCES

1. Hasiguti, R. R.; and Ishino, S.: Defect Mobility and Annealing in Irradiated Germanium and Silicon. Seventh International Conference on the Physics of Semiconductors, Radiation Damage in Semiconductors, Vol. 3, P. Baruch, ed., Academic Press, N.Y., 1964, pp. 259-273.

2. Fang, P. H.; and Liu, Y. M.: Temperature Dependence of Radiation Damage in Silicon. Phys. Lett., vol. 20, no. 4, Mar. 1, 1966, pp. 344-346.

3. Fang, P. H.: Thermal Annealing of Radiation Damage in Solar Cells. NASA TM X-55399, 1965.

4. Miller, G. L.; Lang, D. V.; and Kimerling, L. C.: Capacitance Transient Spectroscopy. Annual Review of Materials Science, Vol. 7, R. A. Huggins, ed., Annual Reviews, Inc., 1971, pp. 377-448.

5. Lee, Y. H.; et al.: EPR and Transient Capacitance Studies on Electron-Irradiation Silicon Solar Cells. Solar Cell High Efficiency and Radiation Damage, NASA CP-2020, 1977, pp. 179-186.

6. Lee, Y. H.; Corbett, J. W.; and Browner, K. L.: EPR of a Carbon-Oxygen-Divacancy Complex in Irradiated Silicon. Phys. Stat. Sol., A, Vol. 41, 1977, pp. 637-647.

7. Mooney, P. M.; et al.: Defect Energy Levels in Boron-Doped Silicon Irradiated with 1-MeV electrons. Phys. Rev. B, vol. 15, no. 8, Apr. 15, 1977, pp. 3836-3843.

8. Rozenzweig, W.: Diffusion Length Measurements by Means of Ionizing Radiation. Bell Syst. Tech. J., vol. 41, no. 5, Sept. 1962, pp. 1573-1588.

9. Hall, R. N.: Electron-Hole Recombination in Germanium. Phys. Rev., vol. 87, no. 2, July 15, 1952, p. 387.

10. Shockley, W.; and Read, W. T., Jr.: Statistics of the Recombinations of Holes and Electrons. Phys. Rev., vol. 87, no. 5, Sept. 1, 1952, pp. 835-842.

11. Srour, J. R.; et al.: Radiation Effects on Semiconductor Materials and Devices. NRTC-73-46 R, Northrup Corp., 1973, p. 126. (HDL-TR-171-4, AD-776420)

12. Kimerling, L. C.: Defect States in Electron-Bombarded Silicon: Capacitance Transient Analysis. Radiation Effects in Semiconductors, N. B. Urli and J. W. Corbett, eds., Institute of Physics Conference Series No. 31, Institute of Physics (London), 1977, pp. 221-230.

TABLE I. - CAPTURE CROSS SECTIONS FROM DLTS

DEFECT ENERGY LEVEL (eV)	CAPTURE CROSS SECTIONS (cm^2)	
	σ_P	σ_N
E_V+0.38	$2x10^{-16}$	--
E_C-0.27	--	$2x10^{-13}$
E_V+0.23	$3x10^{-16}$	--
E_V+0.30	$2x10^{-16}$	--
E_V+0.26	--	--
E_V+0.2	--	--

TABLE II. - ELECTRON CAPTURE CROSS SECTIONS

ENERGY LEVEL OF DEFECT eV	ELECTRON CAPTURE CROSS SECTION (cm^2)	METHOD FOR OBTAINING CROSS SECTION
E_C-0.27	$2x10^{-13}$	DLTS
E_V+0.38	$3x10^{-14}$	*$\sigma_N/\sigma_P \sim 150$
E_V+0.23	$3.9x10^{-13}$	*$\sigma_N/\sigma_P \sim 1300$
E_V+0.30	$3.6x10^{-13}$	FIT OF $\frac{1}{L^2}$ RATIO TO DLTS (250° C)
E_V+0.26	$9.5x10^{-14}$	FIT OF $\frac{1}{L^2}$ RATIO TO DLTS (300° C)

*COMPUTED FROM σ_N/σ_P RATIOS FOR 1.5 Ω-cm P-TYPE (FZ) FROM SROUR, CURTIS, OTHMER, CHIU & DEOKAR: REPORT HDL-TR-171-4-U.S. ARMY

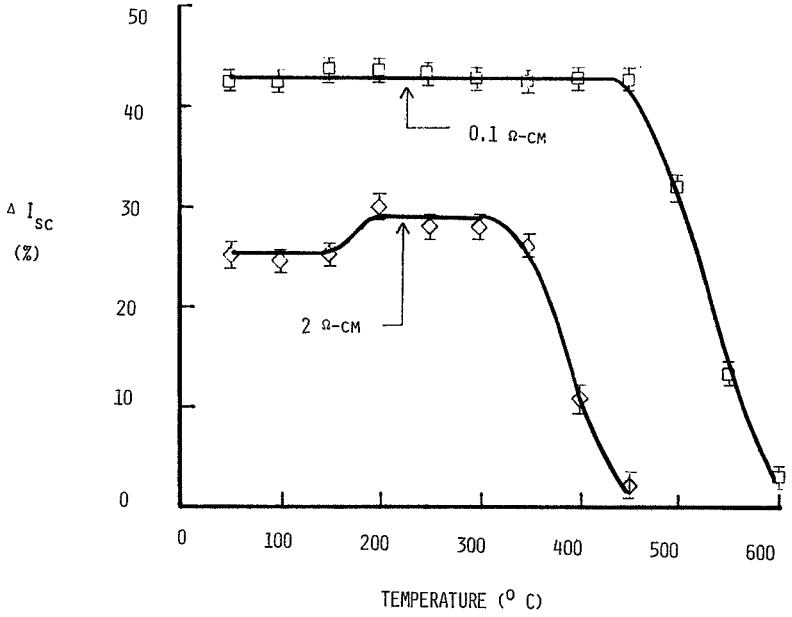

Figure 1. - Isochronal anneal of n^+p silicon solar cells after 1-MeV-electron irradiation. $\varphi = 10^{15}/cm^2$; time at temperature, 20 min.

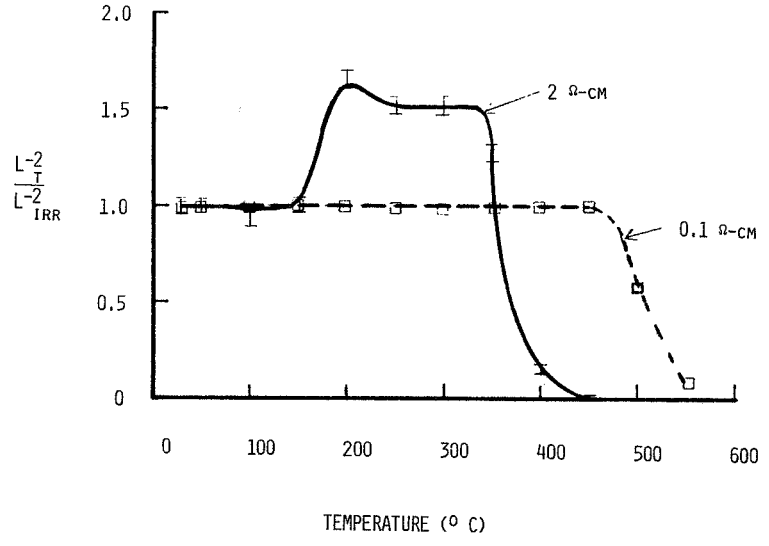

Figure 2. - $1/L^2$ ratios from diffusion lengths measured during isochronal anneal.

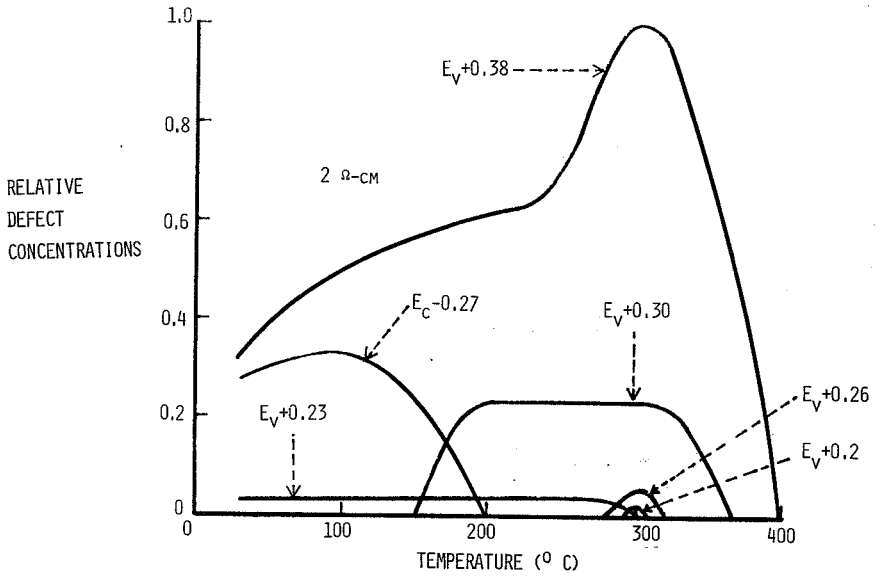

Figure 3. - Relative defect concentrations from DLTS.

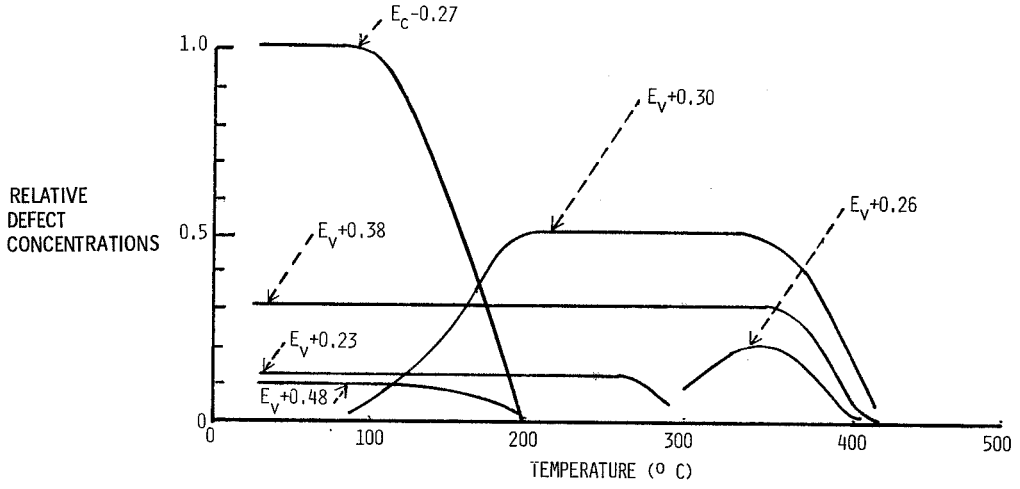

Figure 4. - DLTS data for 0.3 ohm-cm P-Si.

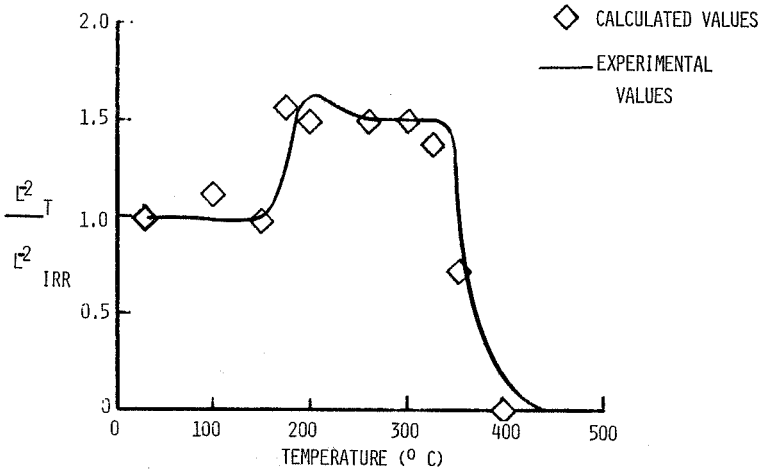

Figure 5.- Calculated and measured $1/L^2$ ratios for 2 ohm-cm cells.

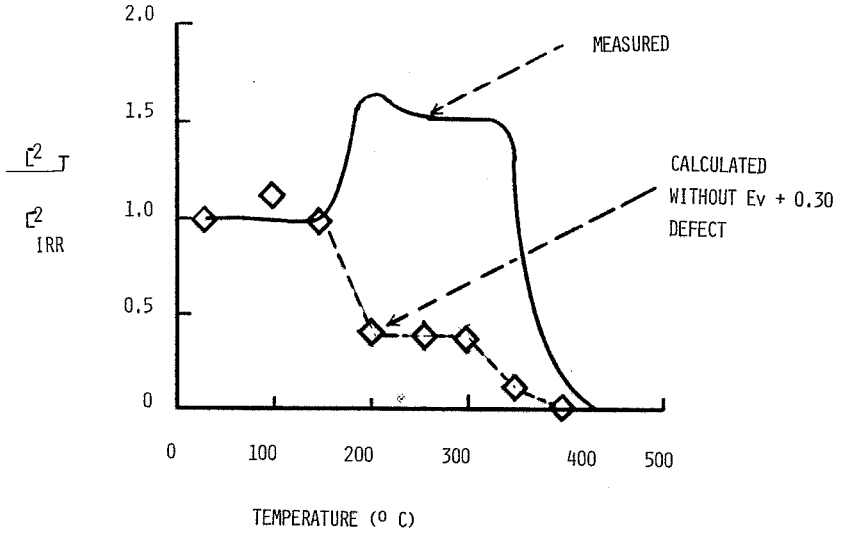

Figure 6.- Calculated and measured $1/L^2$ ratios, omitting E_v + 0.30 effect.

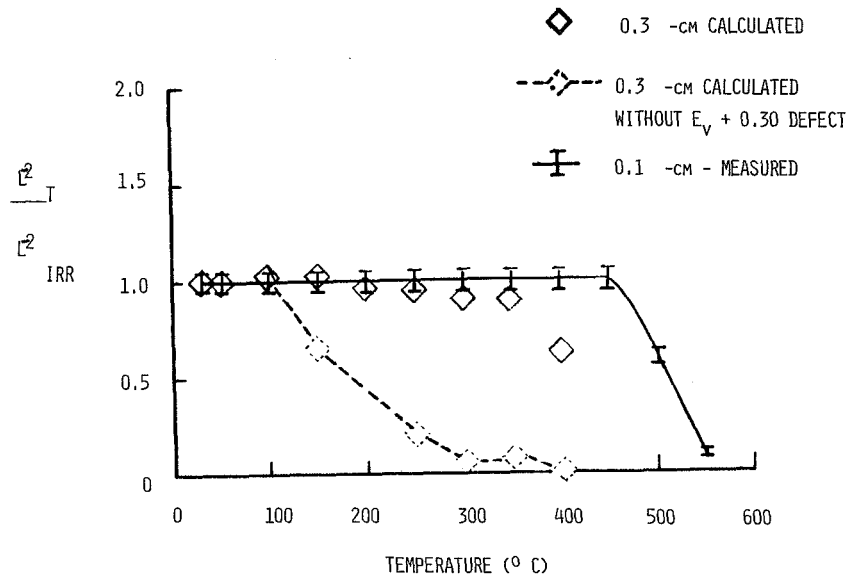

Figure 7. - Calculated and measured $1/L^2$ ratios for low-resistivity P-Si.